

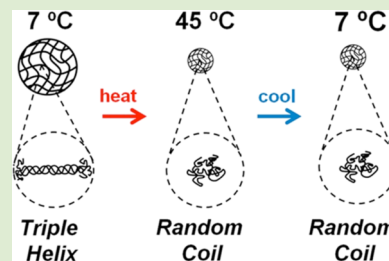
# Thermoresponsive Gelatin Nanogels

Sahil Sandesh Gandhi, Huan Yan, and Chanjoong Kim\*

Chemical Physics Interdisciplinary Program and Liquid Crystal Institute, Kent State University, P.O. Box 5190, Kent, Ohio 44242, United States

## Supporting Information

**ABSTRACT:** We present a novel tunable thermoresponsive gelatin nanogel that shows a volume transition at  $\sim 32$  °C. A thermally induced volume reduction of more than 30 $\times$  is observed due to the helix to random coil transition of gelatin chains confined in the nanogels. The physical process and key factors influencing thermoresponsive properties are investigated using dynamic light scattering (DLS), transmission electron microscopy (TEM), and polarimetry. The thermoresponsive properties of this nanogel can be exploited in the development of new types of stimuli-responsive, biomedically relevant materials based on natural polymers.



Smart polymer nanogels, which are chemically cross-linked nanoparticles swollen in water, have gained considerable attention due to their unique properties tailored from the combination of stimuli-responsiveness and nanoscale size in a single material system.<sup>1</sup> This system holds great potential for use in biomedical applications such as controlled drug release, tissue engineering, biosensors, etc.<sup>2–4</sup> However, the concentration, time and temperature-dependent cytotoxicity of well-known thermosensitive polymers such as cross-linked poly(*N*-isopropylacrylamide) (pNIPAM) poses limitations on their use for *in vivo* applications.<sup>5</sup> Hence, in the past three decades, significant efforts have been devoted to the synthesis and application of biopolymeric nanoparticles for controlled drug delivery.<sup>6–17</sup> Gelatin nanoparticles can be attractive candidates as drug carriers due to their biodegradability and biocompatibility. In the past, emphasis has been placed on utilizing the biodegradable nature of gelatin for cellular uptake and controlled drug delivery.<sup>18–20</sup> Despite the progresses made in this field, to the best of our knowledge, the inherent thermoresponsiveness of gelatin has not been systematically exploited to develop smart gelatin nanogels.

When an aqueous gelatin solution is heated above the helix melting temperature ( $\sim 32$  °C), the gelatin chains become disordered random coils and upon cooling, a part of the gelatin chains can revert to the triple-helical state. The degree of reversion to the helical state depends upon various factors such as concentration, temperature, stress, solvent, and the presence of chemical cross-linking agents.<sup>21–25</sup> This transition has been observed in bulk gelatin solutions and well documented in several investigations in the past few decades.<sup>26–28</sup> Even in chemically cross-linked gelatin gels, the formation of triple helical structures is allowed at low temperatures, if the chemical cross-linking density is low.<sup>29,30</sup> Therefore, we hypothesize that thermoresponsiveness may be realized in nanoscale gelatin particles based on the following reasoning. If optimally chemically cross-linked, gelatin nanogels would allow the formation of semiflexible, relatively stiff “worm-like” helical

structures at low temperatures. These helical structures may undergo a transition to disordered random coils, thereby imparting a shorter persistence length and higher flexibility to the polymer chains, leading to deswelling or shrinking of the nanoparticles.

This letter presents, for the first time, thermoresponsive gelatin nanogels that show a volume transition at the helix-melting temperature, and the molecular mechanism behind the volume transition. Using dynamic light scattering (DLS), transmission electron microscopy (TEM), and polarimetry, we study how temperature changes affect the particle size and the molecular configuration of smart gelatin nanogels and determine key factors influencing the thermoresponsive properties. The volume transition temperature of our nanogel is surprisingly close to that of pNIPAM, that is, around the body temperature.<sup>31–34</sup> This novel smart nanogel is very promising for the development of advanced biomedical materials.

In 1978, Marty and co-workers<sup>7</sup> first reported a desolvation approach for the fabrication of gelatin nanoparticles. It involves the dropwise addition of a desolvating agent such as sodium sulfate or acetone to a gelatin solution, leading to the coacervation of gelatin chains. Upon reaching the critical level of coacervation, the coacervate is redissolved by the addition of isopropanol and cross-linking is initiated by the addition of glutaraldehyde. Since then, desolvation has been one of the most commonly used approaches for the preparation of gelatin nanogels, sometimes with modifications such as those reported by Coester and co-workers<sup>8,16</sup> and Azarmi and co-workers<sup>9</sup> who introduced a second desolvation step. Several pharmaceutical scientists have used desolvation methods for the preparation of gelatin nanoparticles employed in controlled drug delivery.<sup>8–10,16,17</sup> However, the influence of important

Received: August 14, 2014

Accepted: October 15, 2014

Published: November 7, 2014



reaction parameters, namely, cross-linking time, cross-linking temperature, and concentration of cross-linking agent on the properties of gelatin nanogels has received little attention. We prepare gelatin nanogels via a one-step desolvation approach at various cross-linking conditions (time, temperature, and cross-linker concentrations) in order to find optimized ones that allow the formation of helical structures over the course of the preparation. To avoid confusion, we make a distinction between the cross-linking ( $T_x$ ) and the environmental temperature ( $T_e$ ), that is, the temperature at which characterization experiments are performed. After gelatin chains are chemically cross-linked for a given cross-linking time ( $t$ ), the reaction is quenched using sodium metabisulfite. The quenched mixture is then stirred at  $T_x$  for 90 min to promote the formation of helical structures. It is important to note that the concentration of the cross-linking agent used in our modified approach is 4-fold lower than that used in previous works.<sup>9,10,16,17</sup> DLS is used to measure particle sizes and size distributions at  $T_e$  ranging between 7 and 45 °C. Both heating and cooling scans are performed to determine if the nanogel exhibits a reversible thermoresponsive volume transition.

The  $T_e$ -induced size changes in nanogels prepared at different  $T_x$  and  $t$  are shown in Figure 1. To the best of our

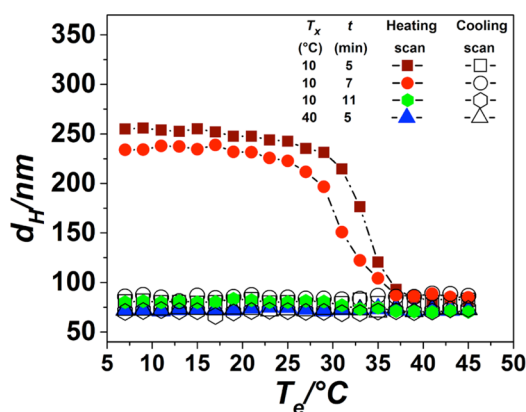


**Figure 1.** Environmental temperature ( $T_e$ ) dependence of the average hydrodynamic diameter ( $d_H$ ) of nanogels prepared at different cross-linking temperatures ( $T_x$ ) and cross-linking times ( $t$ ). The standard deviation is no more than 8 nm. The solid and hollow symbols correspond to heating and cooling scans, respectively.

knowledge, this is the first observation of a thermally induced volume transition of gelatin nanoparticles. Nanogels that are cross-linked at a lower  $T_x$  for a shorter  $t$  exhibit a volume transition during  $T_e$  increase. The particle size (average hydrodynamic diameter,  $d_H$ ) of the nanogel cross-linked at 10 °C for 5 min drops from  $\sim 260$  to  $\sim 80$  nm as  $T_e$  is raised from 7 to 45 °C. In order to verify the DLS size change is not any artifact, we take TEM images of the nanogel cross-linked at 10 °C for 5 min in order to verify the  $T_e$ -dependence of the size. TEM samples are prepared from a dilute nanogel suspension maintained at 7 °C and one warmed up to 45 °C. Figure 2 clearly demonstrates that there is a real size change with the variation of  $T_e$ . One may notice that the size of gelatin nanoparticles in the TEM image at each corresponding  $T_e$  is smaller than the average hydrodynamic diameter from the DLS measurement (Figure 1), but the size discrepancy is simply because the TEM samples are dried while the DLS samples are in a swollen state. Nanogels cross-linked at the same temperature (10 °C), but for a longer  $t$  (7 min), also display

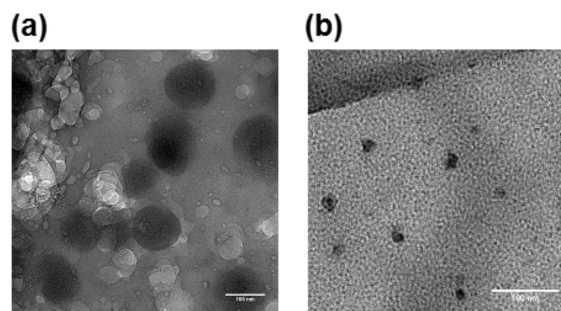


**Figure 2.** TEM images of the gelatin nanogel cross-linked at 10 °C for 5 min. TEM samples are prepared from a dilute nanogel suspension maintained at (a) 7 °C and one warmed up to (b) 45 °C.

a similar degree of size reduction ( $\sim 230$  nm to  $\sim 80$  nm) upon the rise of  $T_e$ . The transition temperature for both nanogels is  $\sim 32$  °C and is close to the body temperature (37 °C). Nanogels cross-linked at a higher  $T_x$  (40 °C) or for a longer  $t$  (11 min), which are comparable to the nanogel preparation conditions of previous works,<sup>8–10,16,17</sup> do not exhibit the thermoresponsive behavior displayed by the nanogels cross-linked at 10 °C for 5 or 7 min shown above. When  $T_x$  is 40 °C, the resulting nanogels consist of only cross-linked random coils with no helices. Therefore, they do not show the thermoresponsiveness during both heating and cooling scans. The nanogel prepared at a low  $T_x$  of 10 °C but for a longer  $t$  of 11 min does not display temperature-responsiveness, either. This lack of temperature-responsiveness may be due to a higher chemical cross-linking density resulting from the longer  $t$ , thus, leading to a tight network that does not allow helix formation during the 90 min stirring step.

It is important to note that the observed volume transition in the nanogels is irreversible, such that the particle size remains unchanged when  $T_e$  is lowered back to 7 °C. We maintain the temperature of the nanogel at 7 °C for 12 h and observe no further change in  $d_H$ . The particle size remains unchanged even as we perform a second heating scan. Thus, we are certain that the waiting time does not influence the size irreversibility. The nanogels display the same particle size, stability, and thermoresponsive behavior even after 30 days since preparation.

Our proposed mechanism of the irreversible volume transition is schematically illustrated in Figure 3: a helix to random coil transition during heating and a “prohibited”

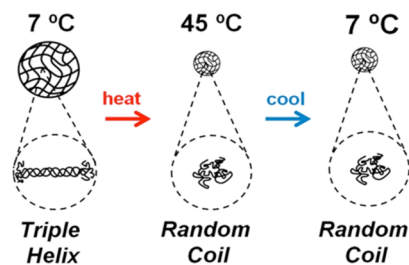


**Figure 3.** Schematic illustration of thermally induced volume transition of loosely cross-linked gelatin nanoparticles. The gelatin chains are assembled to semiflexible, triple-helical structures at low  $T_e$ , which change to flexible, disordered random coils as  $T_e$  is increased higher than the helix–coil transition temperature. A reversion to the helical state upon cooling is “prohibited” due to the presence of chemical cross-links in the system.

random coil to helix transition during cooling of a nanogel. In order to verify this mechanism, we measure the optical rotation of the gelatin nanogel suspensions. Gelatin solutions are known to be optically active when they have helical structures which rotate the plane of polarized light.<sup>21,27</sup> Therefore, when gelatin nanogels undergo a helix to coil transition with a  $T_e$  increase, their optical activities should decrease. If all helices in a nanogel are converted into random coils, the optical activity may decrease down to zero. Using a disc polarimeter, we measure the optical rotation  $\alpha$  of the gelatin nanogels at  $T_e$  ranging between 5 and 55 °C and estimate the specific rotation,  $[\alpha] = \alpha/(l \times c)$ ,<sup>27</sup> where  $l$  is the path length of the sample tube and  $c$  is the concentration of the nanogel. The  $T_e$ -dependent specific rotations of the nanogels prepared at different  $T_x$  and  $t$  are shown in Figure 4. The specific rotations of the nanogels show

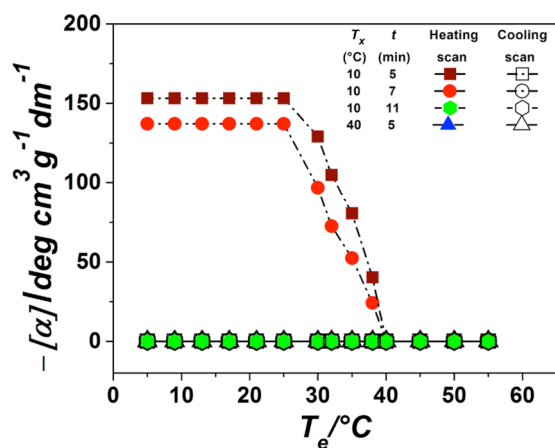


**Figure 4.** Specific rotation  $[\alpha]$  as a function of  $T_e$  of nanogels prepared at different cross-linking temperatures ( $T_x$ ) and cross-linking times ( $t$ ). The standard deviation is 5 deg cm<sup>3</sup> g<sup>-1</sup> dm<sup>-1</sup>. The solid and hollow symbols correspond to heating and cooling scans, respectively.

trends similar to the DLS results: those prepared at  $T_x = 10$  °C for shorter times show an irreversible decrease with increasing  $T_e$ , indicating an irreversible helix to random coil transition, while those cross-linked for a longer time (11 min) or prepared at  $T_x = 40$  °C show no change in  $[\alpha]$ . At low  $T_e$ , the nanogels cross-linked at 10 °C for 5 min have a higher value of  $[\alpha]$  than the nanogels cross-linked at 10 °C for 7 min. A shorter  $t$  may lead to a lower chemical cross-linking density and, consequently, a higher fraction of helical structures, resulting in higher  $[\alpha]$  and larger particle size as evident in the DLS results (Figure 1).  $[\alpha]$  of the nanogels cross-linked at a lower temperature for shorter times goes down to zero at higher  $T_e$ , indicating a complete transition of helices to random coils. Nanogels prepared at longer reaction time ( $t = 11$  min,  $T_x = 10$  °C) or for higher temperature ( $T_x = 40$  °C,  $t = 5$  min) show no optical rotation during heating or cooling. This confirms our hypothesis that there is no helix formation during the preparation of these nanogels.

We believe that the primary reason for thermoresponsiveness having not been reported in previous works on gelatin nanogels is because  $T_x$ ,  $t$ , and the concentration of the cross-linking agent were too high for gelatin chains in nanogels to form and retain helical conformations. Thus, the nanogels prepared in previous works may have consisted of tightly cross-linked random coils, which lack the flexibility to allow the formation of triple helical structures. We note that when  $t$  is shorter than 5 min, it is hard

to obtain nanogels due to the problem of aggregation (the success rate <50%), and moreover, the obtained ones do not display thermoresponsive behavior (constant particle size and optical rotation). The lack of thermoresponsiveness at  $t < 5$  min may be because the elastic force that depends on cross-linking density is too weak to pull random coils together even at higher temperatures.<sup>35</sup> Thus, there is only a small window of optimum cross-linking and stirring conditions via which thermoresponsive nanogels can be reproducibly prepared.

It is important to note that the particle size of the nanogels is influenced by the applied shear rate (stirring rate) during preparation and what stage of the preparation process shear is applied at. We believe that shear leads to stretching and alignment of the gelatin chains, thus, making partial renaturation of the gelatin chains in the nanoconfined environment easier.<sup>36</sup> We verify this by stopping stirring after quenching the cross-linking reaction and merely maintaining the mixture at 10 °C under zero shear for 90 min. This results in nonresponsive nanogels with a particle size of ~80 nm and no optical activity. This result indicates that helix formation takes place during the 90 min of stirring after quenching the cross-linking reaction. This argument is further supported by the results in Figure 4 which shows that the specific rotation goes down to zero due to complete melting of the helices as  $T_e$  is increased to 40 °C. If helix formation takes place before the initiation of cross-linking, the initially formed helices would be fixed in place due to chemical cross-links and their unfolding upon raising  $T_e$  to 40 °C would be prevented. In that case, one would expect the nanogel to exhibit a latent optical activity due to these permanent residual initial helices. In fact, we have observed such a behavior in higher preshear tests and also noticed that the particle size decreases as the stirring rate during the last 90 min of stirring is lowered (data not shown).

We attribute the irreversibility of thermoresponsiveness in the gelatin nanogels to the low effective concentration of gelatin in each nanogel since triple helix formation without shear alignment requires concentration higher than the critical gelation concentration (~1%).<sup>24,27</sup> In previously studied bulk gelatin gels, the triple helices can form reversibly without shear because the concentration of gelatin was high (~10%).<sup>29,30</sup> This led us to investigate whether the application of shear can also result in a reversion of the particle size of the deswollen nanogels that have been heated higher than the volume transition temperature. As described above, the nanogel cross-linked for 5 min at 10 °C shrinks from an initial particle size ~260 nm to ~80 nm upon the rise of  $T_e$  to 45 °C due to a thermally induced volume transition. We then proceed to lower  $T_e$  to 10 °C and stir the nanogel at 1600 rpm for 990 min (16.5 h) in a 100 mL round-bottom flask, while monitoring the particle size every 90 min. The average particle size steadily increases with the stirring time until it reaches a plateau value of ~200 nm, as shown in Figure 5a. This sheared nanogel again undergoes a thermally induced volume transition when  $T_e$  is raised to 45 °C, as shown in Figure 5b. Thus, we conclude that while the volume transition displayed by gelatin nanogels cannot be reversed simply by lowering  $T_e$ , a partial reversion can be induced by the application of shear at a low temperature for a long time. The responsiveness of these nanogels to shear forces may provide a useful means for deciphering the mechanical responses of biomolecules in biological environments, where force generation by cells plays an important role.<sup>37</sup> The effects of applied shear rates and stresses on the



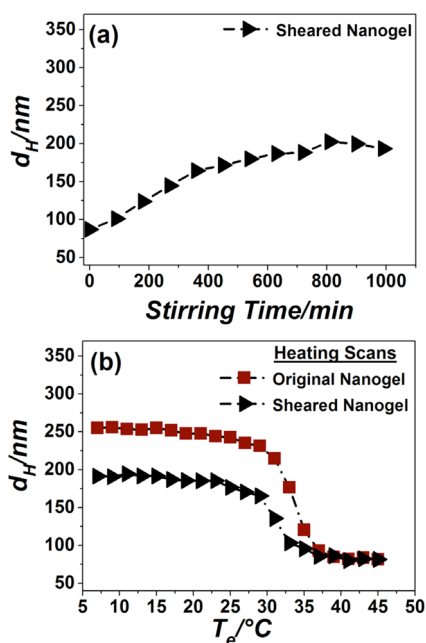


**Figure 5.** (a) Stirring time dependence of the average hydrodynamic diameter ( $d_H$ ) of a nanogel cross-linked at 10 °C for 5 min that has undergone deswelling due to the heating and cooling scans (7 → 45 → 7 °C) shown in Figure 1. Stirring the deswollen nanogel at 1600 rpm at  $T_e = 10$  °C for 990 min (16.5 h) results in a partial recovery of the particle size (from ~80 to ~200 nm). (b) The  $T_e$ -dependence of  $d_H$  during a heating scan of the original nanogel just after preparation and one that has partially regained its particle size after the 990 min stirring of (a). The standard deviation is no more than 8 nm.

thermoreponsive properties of gelatin nanogels will be addressed in detail in our next publication.

In summary, we report tunable thermoresponsive gelatin nanogels that display a volume transition at ~32 °C due to the helix to random coil transition. This novel helix-melting mechanism is markedly different from the reversible random coil to globule transition that occurs at the lower critical solution temperature (LCST) in popular thermosensitive polymers like pNIPAM.<sup>31–34</sup> The deswelling during a coil to globule transition is a result of reduced polymer–solvent interaction above the LCST, while that in gelatin nanogels may occur due to the reduction of the end-to-end distance between two cross-links during the helix to coil transition. The key to our approach is the optimization of the cross-linking conditions so as to yield nanogels that contain helices. This stimuli-responsive behavior of the nanogels may have fundamental implications in the physical responses of biopolymers under nanoconfinement. Our approach may also be exploited to develop new types of stimuli-responsive materials based on other helix forming polymers such as polypeptides, DNA, xanthane, and PEG-based block copolymers.<sup>24,25,38–42</sup> These smart bionanogels with stimuli-responsiveness, biodegradability, and low cytotoxicity may lead to various biomedical applications such as controlled drug and gene delivery and biosensors.

## EXPERIMENTAL SECTION

**Preparation of Gelatin Nanogels.** Three nanogels were prepared at  $T_x = 10$  °C for  $t = 5, 7,$  and 11 min via a one-step desolvation technique. A nanogel was also prepared at  $T_x = 40$  °C for 5 min. Gelatin Type A (Amresco, Solon, OH) was used for the synthesis of

nanogels. Glutaraldehyde (Sigma-Aldrich, St. Louis, MO) was used as the cross-linking agent. Gelatin stock solution (2 mL, 5%) and sodium acetate solution (1 mL, 16.5%) were dissolved in distilled water (7 mL) in a 40 mL vial (internal diameter ≈ 25 mm) by stirring with a stirring bar (length ≈ 25 mm) for 10 min at 600 rpm under constant heating in an oil bath at 40 °C with the addition of Tween-20 surfactant (100 μL). The vial was taken out of the oil bath and the desolvation process was induced by the dropwise addition of sodium sulfate solution (6.5 mL, 20%) while stirring at 600 rpm, obtaining a faint turbidity due to the coacervate phase. The coacervate was redissolved by the addition of isopropanol (1.3 mL) until a clear solution was obtained. In the case of  $T_x = 10$  °C, the temperature of the solution was lowered to 10 °C using an ice bath. After stirring at 1600 rpm for 5 min, glutaraldehyde solution (400 μL, 6.25%) was added while still stirring at the same speed for  $t$  specified above. The cross-linking reaction was quenched by the addition of sodium metabisulfite (5 mL, 12%) enough to seize all unreacted glutaraldehyde and ensure low cytotoxicity.<sup>43</sup> The nanogels were cleaned by dialyzing the final clear solutions against distilled water for 48 h.

**Characterization of Gelatin Nanogels.** The dynamic light scattering setup of a ZetaPlus Zeta Potential Analyzer (Brookhaven Instruments Corporation) equipped with a 35 mW solid state laser (red, 660 nm wavelength) was used to measure the temperature-dependent sizes and size distributions of gelatin nanoparticles. Particle diameters were measured at  $T_e$  varying from 7 to 45 °C (heating scan) and down back to 7 °C (cooling scan). Gelatin nanoparticles maintained at  $T_e = 7$  °C and those warmed up to 45 °C were imaged using a transmission electron microscope (TEM, FEI Tecnai F20). The TEM samples were prepared by drying dilute suspensions of nanogels on copper grids in a hood. The optical rotation of gelatin nanogels was measured at various  $T_e$  between 5 and 55 °C using a WXG-4 disc polarimeter with a 589 nm sodium lamp and a sample path length of 20 cm. The temperature of the sample tube was controlled using a benchtop temperature controller (Omega Technologies, CSC32 series).

## ASSOCIATED CONTENT

### Supporting Information

The evolution of  $d_H$  measured at 7 °C as a function of cross-linking time ( $t$ ) is shown in Figure S1. This material is available free of charge via the Internet at <http://pubs.acs.org>.

## AUTHOR INFORMATION

### Corresponding Author

\*E-mail: [ckim9@kent.edu](mailto:ckim9@kent.edu).

### Notes

The authors declare no competing financial interest.

## ACKNOWLEDGMENTS

The authors gratefully acknowledge the technical assistance provided by Dr. Baekkyoung Sung, Anshul Sharma, Priyanka Nalawade, and MinSu Kim. The TEM images were obtained at the Cryo-TEM facility at the Liquid Crystal Institute, Kent State University, supported by the Ohio Research Scholars Program Research Cluster on Surfaces in Advanced Materials. The authors thank Dr. Min Gao for technical support with the TEM experiments. This research was financially supported by the Kent State University start-up fund.

## REFERENCES

- (1) Hamidi, M.; Azadi, A.; Rafei, P. *Adv. Drug Delivery Rev.* **2008**, *60*, 1638–1649.
- (2) Stuart, M. A. C.; Huck, W. T.; Genzer, J.; Müller, M.; Ober, C.; Stamm, M.; Minko, S. *Nat. Mater.* **2010**, *9*, 101–113.

- (3) Alarcón, C. H.; Pennadam, S.; Alexander, C. *Chem. Soc. Rev.* **2005**, *34*, 276–285.
- (4) Ballauff, M.; Lu, Y. *Polymer* **2007**, *48*, 1815–1823.
- (5) Vihola, H.; Laukkanen, A.; Valtola, L.; Tenhu, H.; Hirvonen, J. *Biomaterials* **2005**, *26*, 2055–2064.
- (6) Oppenheim, R. C.; Stewart, N. F. *Drug Dev. Ind. Pharm.* **1979**, *5*, 563–571.
- (7) Marty, J. J.; Oppenheim, R. C.; Speiser, P. *Pharm. Acta Helv.* **1978**, *53*, 17–23.
- (8) Coester, C. J.; Langer, K.; von Briesen, H.; Kreuter, J. *J. Microencapsul.* **2000**, *17*, 187–193.
- (9) Azarmi, S.; Huang, Y.; Chen, H.; McQuarrie, S.; Abrams, D.; Roa, W.; Löbenberg, R. *J. Pharm. Pharm. Sci.* **2006**, *9*, 124–132.
- (10) Vandervoort, J.; Ludwig, A. *Eur. J. Pharm. Biopharm.* **2004**, *57*, 251–261.
- (11) Weber, C.; Coester, C.; Kreuter, J.; Langer, K. *Int. J. Pharm.* **2000**, *194*, 91–102.
- (12) Sundar, S.; Kundu, J.; Kundu, S. C. *Sci. Technol. Adv. Mater.* **2010**, *11*, 014104.
- (13) Ofokansi, K.; Winter, G.; Fricker, G.; Coester, C. *Eur. J. Pharm. Biopharm.* **2010**, *76*, 1–9.
- (14) Balthasar, S.; Michaelis, K.; Dinauer, N.; von Briesen, H.; Kreuter, J.; Langer, K. *Biomaterials* **2005**, *26*, 2723–2732.
- (15) Curcio, M.; Altimari, I.; Spizzirri, U. G.; Cirillo, G.; Vittorio, O.; Puoci, F.; Iemma, F. *J. Nanopart. Res.* **2013**, *15*, 1–11.
- (16) Coester, C.; Nayyar, P.; Samuel, J. *Eur. J. Pharm. Biopharm.* **2006**, *62*, 306–314.
- (17) Leo, E.; Vandelli, M. A.; Cameroni, R.; Forni, F. *Int. J. Pharm.* **1997**, *155*, 75–82.
- (18) Schwick, H. G.; Heide, K. *Bibl. Haematol.* **1968**, *33*, 111–125.
- (19) Ward, A. G.; Courts, A. *Science and Technology of Gelatin*; Academic Press: New York, 1977.
- (20) Zwioerek, K.; Kloeckner, J.; Wagner, E.; Coester, C. *J. Pharm. Pharm. Sci.* **2004**, *7*, 22–8.
- (21) Gornall, J. L.; Terentjev, E. M. *Soft Matter* **2008**, *4*, 544–549.
- (22) Harrington, W. F.; Rao, N. V. *Biochemistry* **1970**, *9*, 3714–3724.
- (23) Hauschka, P. V.; Harrington, W. F. *Biochemistry* **1970**, *9*, 3734–3745.
- (24) Courty, S.; Gornall, J. L.; Terentjev, E. M. *Biophys. J.* **2006**, *90*, 1019–1027.
- (25) Tamashiro, M. N.; Pincus, P. *Phys. Rev. E* **2001**, *63*, 021909.
- (26) Brown, F. R., III; Hopfinger, A. J.; Blout, E. R. *J. Mol. Biol.* **1972**, *63*, 101–115.
- (27) Djabourov, M.; Leblond, J.; Papon, P. *J. Phys. (Paris)* **1988**, *49*, 319–332.
- (28) Djabourov, M.; Leblond, J.; Papon, P. *J. Phys. (Paris)* **1988**, *49*, 333–343.
- (29) Bode, F.; da Silva, M. A.; Drake, A. F.; Ross-Murphy, S. B.; Dreiss, C. A. *Biomacromolecules* **2011**, *12*, 3741–3752.
- (30) Giraudier, S.; Hellio, D.; Djabourov, M.; Larreta-Garde, V. *Biomacromolecules* **2004**, *5*, 1662–1666.
- (31) Voudouris, P.; Florea, D.; van der Schoot, P.; Wyss, H. M. *Soft Matter* **2013**, *9*, 7158–7166.
- (32) Hashmi, S. M.; Dufresne, E. R. *Soft Matter* **2009**, *5*, 3682–3688.
- (33) Senff, H.; Richtering, W. *J. Chem. Phys.* **1999**, *111*, 1705–1711.
- (34) Lutz, J. F.; Akdemir, Ö.; Hoth, A. *J. Am. Chem. Soc.* **2006**, *128*, 13046–13047.
- (35) Rubinstein, M.; Colby, R. H. *Polymer Physics*; Oxford University Press: U.K., 2003.
- (36) Hoermann, H.; Schlebusch, H. *Biochemistry* **1971**, *10*, 932–937.
- (37) Bao, G.; Suresh, S. *Nat. Mater.* **2003**, *2*, 715–725.
- (38) Vedenov, A. A.; Dykhne, A. M.; Frank-Kamenetskii, M. D. *Phys.-Usp.* **1972**, *14*, 715–736.
- (39) Norton, I.T.; Goodall, D. M.; Frangou, S. A.; Morris, E. R.; A. Rees, D. *J. Mol. Biol.* **1984**, *175*, 371–394.
- (40) Seright, R. S.; Henrici, B. J. *SPE Reservoir Eng.* **1990**, *5*, 52–60.
- (41) Liu, W.; Sato, T.; Norisuye, T.; Fujita, H. *Carbohydr. Res.* **1987**, *160*, 267–281.
- (42) Inomata, K.; Itoh, M.; Nakanishi, E. *Polym. J.* **2005**, *37*, 404–412.
- (43) Jordan, S. L. *J. Toxicol. Environ. Health, Part A* **1996**, *47*, 299–309.